Change of agitation power when emptying the tank for propeller impellers

Jacek Stelmach[a], Czesław Kuncewicz[a] , Tomas Jirout[b], Frantisek Rieger[b]

[a]Lodz University of Technology, Faculty of Process and Environmental Engineering, Wolczanska 213, 93-005 Lodz, ORCID numbers: JS: 0000-0001-9348-5315, CK: 0000-0003-0004-1980,

[b]Czech Technical University in Prague, Faculty of Mechanical Engineering, Technicka 4, 166 04 Praha 6, ORCID numbers: TJ: 0000-0003-3110-6978, FR: 0000-0001-6477-5567

Corresponding author: Jacek Stelmach, jacek.stelmach@p.lodz.pl

Abstract. In this study, the phenomenon of mixing power increase when emptying tanks with an operating propeller impeller was examined. The tests were carried out for impellers with wide and narrow blades in two geometrically similar tanks with diameters $T = 545$ mm and $T = 300$ mm equipped with four standard baffles. The varied mixing power during tank emptying was examined on a larger scale, and on a scale of $T = 300$ mm the distribution of axial and radial velocities in the vertical r - z plane was determined using the PIV system. A very large increase in mixing power was found when the liquid-free surface being lowered was close to the upper surface of the blades. In the limit case, as much as a three-fold increase in mixing power was observed compared to the mixing power in a tank completely filled. It was found that the increase in mixing power was caused by a change in the mode of liquid circulation in the mixing tank when the liquid surface approached the impeller area. Correlation equations determining the values of the mixing power increase factor φ depending on the geometric parameters of the impeller and the Froude number are given. The φ values for propeller impellers were compared with similar values obtained for other types of impellers.

Keywords: propeller impellers, mixing tank hydrodynamics, tank emptying, mixing power increase

1. INTRODUCTION

For agitation in tanks in the turbulent range, various types of turbine agitators are commonly used such as the Rushton impeller with disc (RT impellers), flat blade turbine impellers (FBT), pitched blade turbines (PBTs) and propeller impellers with different blade heights and their inclination angles. RT and FBT impellers are called radial impellers because they mainly eject liquid from their zone in a radial direction. The axial impeller is another type of impeller used for agitation in the range of developed turbulent movement. Due to their streamlined shapes and low energy demand to drive them, they are often used in industrial applications in large tanks. For RT and FBT impellers in the turbulent range the power number Eu is of the order of $Eu \cong 4.5 \div 5.5$, for PBT impellers a similar range is $Eu \cong 0.8 \div 2.5$ while for propeller impellers this range is significantly smaller and amounts to $Eu \cong 0.3 \div 0.8$, depending on the parameters of these impellers. In the limit case, the difference in loads of the motor driving radial and axial impellers can reach ten times higher or more, although on average it is 2 to 4 times higher. Therefore, propeller impellers are often used in large tanks.

Regardless of the popularity of propeller impellers, the number of publications concerning the research on the hydrodynamics of these impellers is relatively small. Extensive research on this subject includes classic work from the 1950s and 1960s, mainly regarding mixing power (Rushton et al., 1950a; Rushton et al.; 1950b, Bates et al., 1963; Landau and Procházka, 1964) and more recent work include studies with a significantly larger research scope (Wylock et al., 2010; Plewik et al., 2010; Furukawa et al., 2012; Reviol et al., 2018a; Reviol et al., 2018b). Furthermore, a great deal of information on mixing power and mixing tank hydrodynamics for propeller impellers can be found in our previous work (Stelmach et al. 2023).

A typical area of application of propeller impellers concerns the mixing of heterogeneous systems, especially liquid-solid suspensions. The liquid stream ejected from the impeller area to the lower part of the tank hits the bottom and simultaneously lifts the solid particles resting there and keeps them in constant suspension (Baresi and Baldi, 1987; Mak, 1992; Sha and Palosaari, 2000; Wang, 2018). For the same reason, propeller impellers are used in crystallization processes (Mersmann, 2001; Plewik et al., 2010; Wylock et al., 2010; Rane et al., 2014), because a stable liquid-solid suspension is obtained at significantly lower energy consumption compared to various types of PBT turbine impellers (Kaćunić et al., 2013).

In industrial conditions, processes can be conducted continuously or periodically. However, even in the case of continuous processes, some preliminary technological operations are also carried out periodically. If the process requires the use of mixing tanks to produce suspensions

2

or emulsions, the tank is most often emptied with a running impeller to ensure constant homogeneity of the mixture during emptying. In the literature on the subject there is evidence that during the production of a suspension in a tank with a large capacity of 300 m³, a significant increase in mixing power demand was observed during tank emptying shortly before the working impeller emerged from the liquid being mixed (Mazoch, 2016), although the first mention about this can be found in Paul's work (Paul et al., 2004). A similar effect of increasing the mixing power during tank emptying was also described in the work of Alberini et al. (2024) and concerned a special design of a paddle impeller placed just above the mixer bottom. The observed increase in mixing power may lead to overload or even burnout of the motor driving the impeller because the motor is usually selected for a filled tank. This is especially dangerous for mixing tanks with capacities of several dozen or more cubic meters of liquid.

The theoretical basics for the increase in mixing power were presented in the works (Stelmach et al., 2021a; Stelmach et al., 2021b) and concerned FBT and PBT impellers: the increase in mixing power occurred only for PBT impellers with axial action where the liquid through the impeller area flowed mainly in a vertical direction. According to these results, when the tank is being emptied, an increase in power always occurred when the height of the liquid layer above the impeller was so small that there were no conditions for the upper part of the rotating circulation loop in the vertical r - z plane to be closed in it. Due to the rotating impeller and the action of centrifugal force, the axial flow of liquid in the area of the impeller had to be changed to radial flow, which is always more energy-consuming than axial flow (Kaćunić et al., 2013). In these specific conditions, the axial impeller had to work for some time as a radial impeller, thus increasing the mixing power, because radial impellers (RT, FBT) require several times greater mixing power than axial impellers (Nagata, 1975; Paul et al., 2004).

Stelmach et al. (2020) also found that for a six-blade 6-PBT turbine impeller with different blade inclination angles α the power increase factor φ depends on the Froude number Fr and the impeller blade inclination angle α according to the correlation equation (1) and in the limit case the mixing power may even double.

$$\varphi = \frac{Eu_{max}}{Eu} = 0.61 \cdot Fr^{-0.285} \cdot (\sin \alpha)^{-0.367} \tag{1}$$

For RLL axial impellers with folding blades (Rieger et al., 2019), which are a variant of PBT impellers, a similar relationship (2) was also obtained. However, for modified RLL MOD impellers (blades ending with an additional vertical element inhibiting the outflow of liquid in the radial direction from the impeller area), relationship (3) was obtained for four apparatus scales from 200 to 400 mm (Rieger et al., 2021). According to equations (1 - 3) in all cases the

power increase factor φ decreased with the increase in the Froude number, and it was independent of the scale of the apparatus.

$$\varphi = \frac{Eu_{max}}{Eu} = 0.510 \cdot Fr^{-0.307} \tag{2}$$

$$\varphi = \frac{Eu_{max}}{Eu} = 0.594 \cdot Fr^{-0.216} \tag{3}$$

Although the power increase when the tank is being emptied occurs only for axial impellers, there are no studies in the literature for the most typical and most common axial impellers, i.e. propeller impellers. The work presented here addresses these gaps, and this will also enable comparison of power increase factors for different types of axial impellers. Two standardized designs of propeller impellers with precisely defined geometric dimensions significantly different in the size of the active surface of the blades were selected as research objects (BN-2472-01:1977; BN-2225-13:1984; Stelmach et al., 2023).

2. MATERIALS AND METHODS

Torque tests conducted while the tank was being emptied were carried out on a quarter-technical scale in a flat-bottomed steel mixing tank with a diameter of $T = 545$ mm, equipped with four standard baffles with a width of $B = 0.1 \cdot D$ and height $H_0 = T = 545$ mm, placed symmetrically around the circumference of the tank (Fig. 1). The tests were conducted on 8 propeller impellers with a diameter of $D = 2 \cdot R_{imp} = 180$ mm ($D/T = 1/3$) with two widths of impeller blades $b = 0.42 \cdot R_{imp}$ and $b = 0.76 \cdot R_{imp}$ (Fig. 2) suspended at a height of $C = T/3$ above the bottom of the mixing tank. For the sake of simplification, the part further below the impeller shown in Fig. 2a will be called "narrow" and the one shown in Fig. 2b "wide". The ratio of the surface areas of the blades of both impellers is relatively high and amounts to 1.87 (Fig. 2c). The variable geometric parameter for both types of impellers is the pitch of the impeller blade $p/D = 0.5, 1.0, 1.5,$ and 2.0. The rotational frequency of the impellers varied within a range of $N = 0.17 \div 5$ s^{-1} ($Re = 5,500 \div 160,000$) and in each case, the impeller pumped the liquid to the bottom of the mixing tank.

Both types of propeller impellers were structures with a variable inclination angle α of the impeller blade depending on the current blade radius R in accordance with equation (4).

$$p = 2 \cdot \pi \cdot R \cdot \tan \alpha \tag{4}$$

The fulfillment of this equation means that for the assumed constant value p, called the pitch of the impeller blade, the inclination angle α decreased with the radius R, and the p/D ratio for a

4

given impeller was constant. Theoretically, in such a case, a stream of liquid with the same axial velocity $U_z = p \cdot N$ will flow out from the impeller zone regardless of the considered radius.
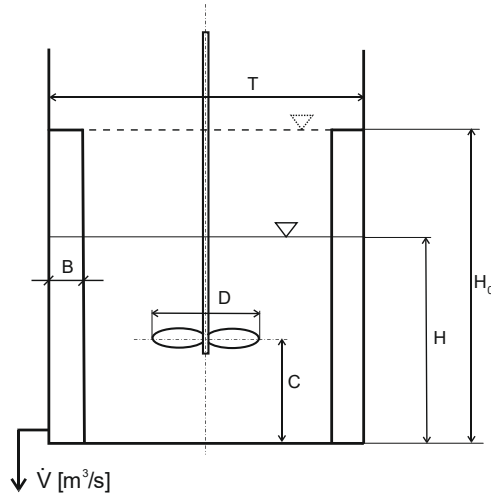

Fig. 1. Diagram of experimental instruments
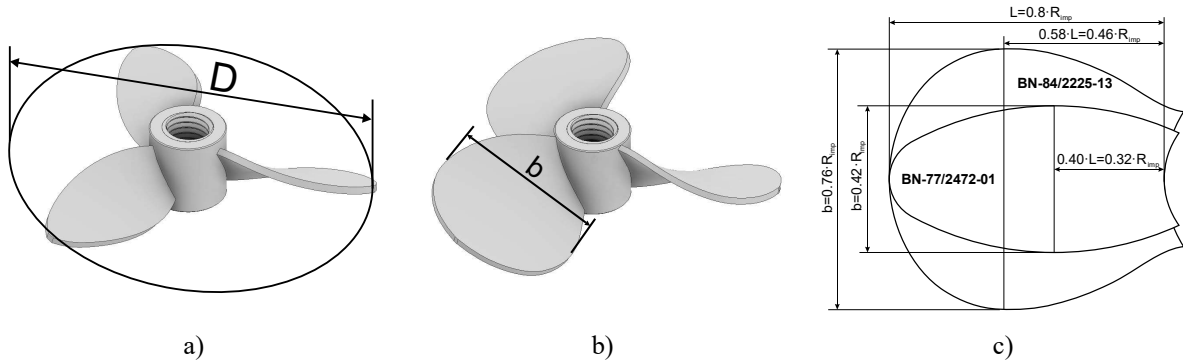

a)   b)   c)

Fig. 2. Propeller impellers narrow (a), wide (b), and blade profiles (c)

Torque measurements were made while the tank was being emptied with an IKA EURO-ST P CV meter. Instantaneous torque values were recorded using the Labworldsoft 4.6 program with an interval of 2 s. A peristaltic pump Verderflex 2010 was used to pump water from the tank. Water from the tank was pumped out through a stub located just above the bottom of the tank. The measurement started by filling the mixing tank with water ($t = 20°C$, $\eta = 1$ mPa·s) to an initial height $H = 330$ mm ($H^* = H/H_0 \cong 0.6$), because preliminary measurements showed that lowering the liquid level in the upper part of the mixing tank hardly changed the torque meter readings. Then the impeller drive was started, and the torque meter and peristaltic pump were turned on. A pump with a constant volumetric flow rate $\dot{V} = 15.6$ ml/s caused the free surface of the liquid in the mixing tank to lower at a rate of 0.176 mm/s. The measurement was finished when the blade of the rotating impeller emerged completely from the water. More details about the measuring instruments can be found in our previous work (Stelmach et al., 2023). No suspension was used in the study, because according to Gzowska's research (Gzowska, 2019), the

mixing power of suspensions with a concentration of up to 8% by mass does not differ significantly from the mixing power of water.

Measurements of the liquid velocity distributions inside the mixing tank for narrow and wide propeller impellers were made in a glass mixing tank with a diameter of $T = 300$ mm, geometrically similar to the mixing tank with a diameter of $T = 545$ mm shown in Fig. 1. Measurements of the axial and radial velocity components were carried out using the PIV technique in the vertical r - z plane placed symmetrically between two adjacent baffles. The mixing tank was additionally placed in a rectangular aquarium filled with distilled water. Technical parameters of the measurement and parameters of the PIV system settings can be found in the work of Stelmach et al. (2021a; 2023).

3. TORQUE MEASUREMENTS

For four selected rotational frequencies of the impeller N, Fig. 3 shows the course of the torque value variations when the tank was being emptied depending on the position of the free surface of the liquid in the mixing tank $H^* = H/H_0$. For the upper part of the mixing tank $H^* = 0.6 \div 0.45$ and different values of the rotational frequency N, straight lines were obtained, although with different slopes. For low rotational frequencies, the M values are practically independent of the liquid level in the mixing tank, while as the N value increases, the torque also increases gradually and, in the limit case, for $N = 2.5$ s^{-1}, the M value increases by up to 20%. However, the increase is not as big as in the case when the liquid-free surface is close to the upper edge of the impeller blades. At this moment, for $H^* \cong 0.45$, there was a key period of very rapid torque increase, and the maximum M value was observed in a narrow range of values of $H^* \cong 0.40 \div 0.44$. For example, for the rotational frequency $N = 1.5$ s^{-1}, this value was $H^* = 0.415$ (see the red line in Fig. 3). The curves of $M = f(H^*)$ for different values of N were, for obvious reasons, shifted relative to each other because in the range of turbulent mixing the torque always increases with an increase in the impeller rotational frequency N ($M \sim N^2$).

After a rather sharp increase in mixing power and with further lowering of the liquid in the mixing tank, the level reaches the height of the upper edge of the blade. The impeller begins to emerge gradually from the liquid, the torque systematically decreases, and when the impeller completely emerges from the liquid the M value is equal or close to zero. It should be noted that a short-term decrease of the impeller torque for the range $H^* \cong 0.44 \div 0.47$, was observed, i.e. just before its rapid increase. It is difficult to explain this phenomenon at present, but it does not in any way affect the selection of the motor power required to drive the impeller.
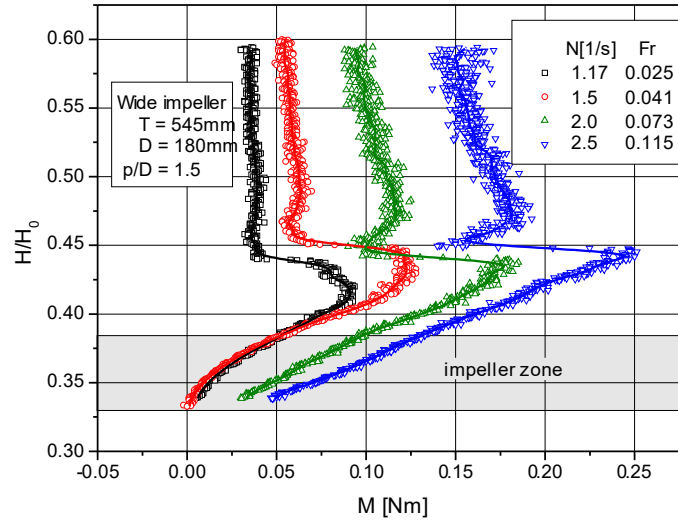
Fig. 3. Torque increase during tank emptying for wide impellers

4. HYDRODYNAMICS IN THE MIXING TANK

The key range of $M = f(H^*)$ variation is that of $H^* = 0.45 \div 0.4$ when there is a sharp increase in torque. It was assumed that the observed increase should be related to the type of liquid circulation in the mixing tank, i.e. to the velocity distribution. Where the rotational frequency of the impeller is constant at $N = 1.5$ s^{-1}, Fig. 4 shows the distribution of liquid velocities in the vertical plane r - z, in a glass mixing tank with a diameter $T = 300$ mm, obtained using the method described in item 2. The measurements were carried out for four heights of the liquid-free surface $H = 150$ mm, 125 mm, 120 mm, and 115 mm. This corresponds to the relative ratios $H^* = 0.45$, 0.42, 0.4, and 0.38. The selected H^* levels at the same time correspond to the area where, as shown in Fig. 3, there is a rapid increase of the torque M. According to Fig. 4, one classic secondary circulation vortex is visible in the mixing tank up to a value of $H^* = 0.50$, the same as for a completely filled tank. The liquid flows through the impeller area in a vertical direction, i.e. the impeller works like a classic axial impeller. However, from the value of $H^* = 0.42$ ($H = 125$ mm), the direction of liquid flow through the impeller area changes from axial to skew flow and then to horizontal radial flow for $H^* = 0.38$. The direction of the liquid rotation also changes from clockwise to counterclockwise. This is the result of the action of centrifugal force and the inability to close the liquid circulation loop above the impeller due to the small volume of the liquid in this space. Changing the flow from axial to radial for the range $H^* = 0.40 \div 0.42$ results in a rapid increase of torque as can be seen in Fig. 3 for the same range (see the red line). For higher rotational frequencies, the change in the nature of the flow is similar, but it occurs for slightly higher values of H^* (Fig. 3).
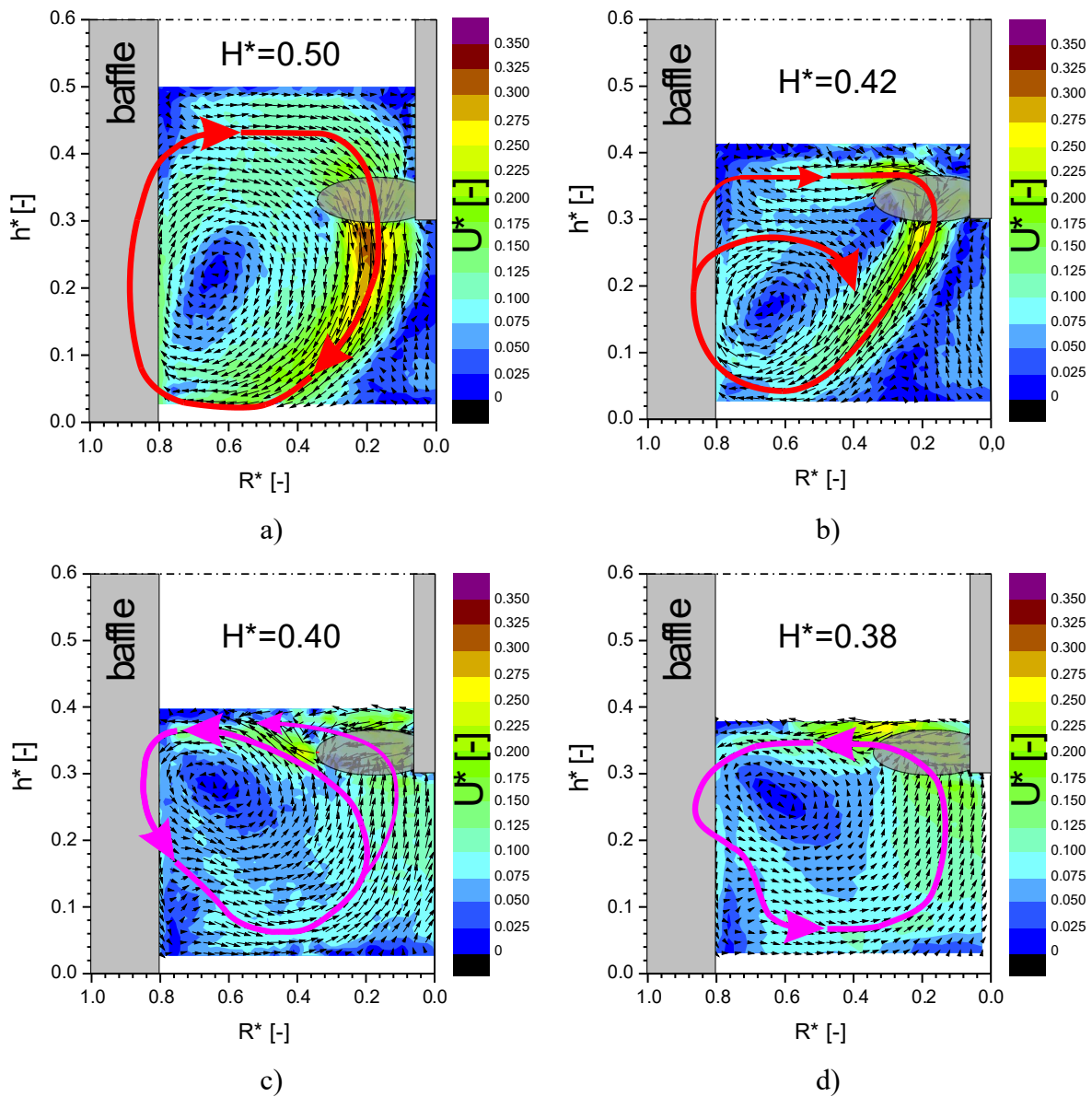
Fig. 4. Velocity distributions in the r - z plane for different liquid levels in the mixing tank, for wide impellers, $T = 300$ mm, $p/D = 1.0$, $N = 1.5$ s^{-1}, $Re = 15\,000$

As it results from the preliminary tests, the velocity of pumping the liquid out of the tank had no effect on the momentary increase in mixing power during emptying the stirred vessel, but it depended primarily on the rotational frequency of the impeller.

5. MIXING POWER INCREASE FACTOR

The waveforms presented in Fig. 3 depend on the rotational frequency of the impeller N. Therefore, Fig. 5 shows the results for the same impeller in the dimensionless system $Eu = f(H^*)$. As can be seen from Fig. 4 the measurement points up to the value of $H^* = 0.45$ approximately coincide and the power number Eu has a constant value of $Eu_0 = 0.81$, as was

obtained for the same impeller in our previous work (Stelmach et al., 2023), in the case when the mixing tank was completely filled to the height $H = H_0$. In order to capture quantitative differences in the mixing power increase, equation (5) was used which defines the mixing power increase factor φ as the ratio of the maximum value of the Euler number Eu_{max} to the value Eu_0 for the same impeller (Stelmach et al., 2021b).

$$\varphi = \frac{Eu_{max}}{Eu_0} \qquad (5)$$

The values of Eu_{max} for individual N values can be read in Fig. 5. The highest values of the φ coefficient were obtained for the lowest rotational frequency $N = 1.17$ s^{-1} and amounted to 2.79 (see legend of Fig. 5). Therefore, in this case, the mixing power increased almost threefold. The smallest increase of 63% was observed for the highest rotational frequency $N = 2.5$ s^{-1}. Such big increases in mixing power are dangerous for the running motor and may lead to its burning out. As can be seen from Fig. 5, the duration of overload is not very long and depends on the size of the tank as well as the speed of its emptying, and for short-term overloads the phenomenon discussed does not have to be dangerous.

In Fig. 5, the great impact of the Froude number on the value of φ_{max} is worth noting. The higher the values of Froude numbers, the lower the values of φ_{max} (see legend of Fig. 5). This means that the greatest motor overloads will occur at low impeller rotational frequencies. This relationship was discussed in more detail in our previous work (Stelmach et al., 2021b).
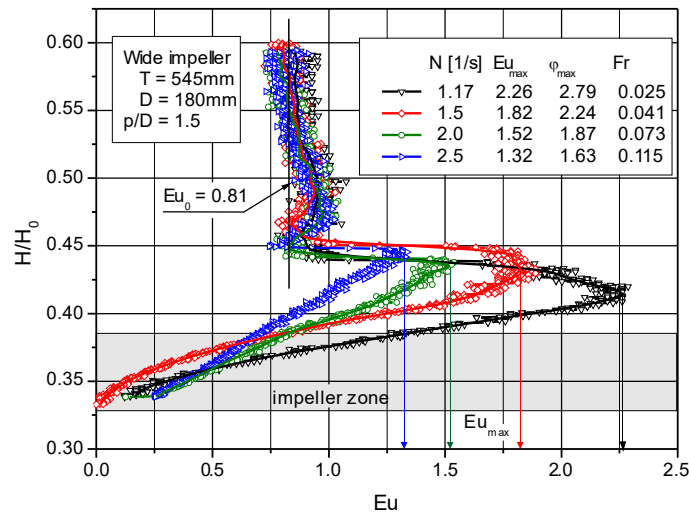

Fig. 5. Euler number increase when emptying the tank for wide impellers

Similarly, Fig. 6 shows the results for a narrow impeller with the same pitch $p/D = 1.5$. Qualitatively, similar results were obtained as in Fig. 5, but they differ significantly in

quantitative terms. For the range $H^* = 0.6 \div 0.45$ one line $Eu_0 = 0.54$ was obtained (Stelmach et al. 2023), the values of the power increase coefficients ranged only from 1.11 to 1.33 depending on the value of N, and these change in the same direction as in Fig. 5. This most probably results from lower values of pumping numbers for narrow impellers (Stelmach et al. 2023). However, the mixing power decrease for $H^* \cong 0.47$ was much more pronounced than in the previous case. It is difficult to explain this phenomenon at the moment.
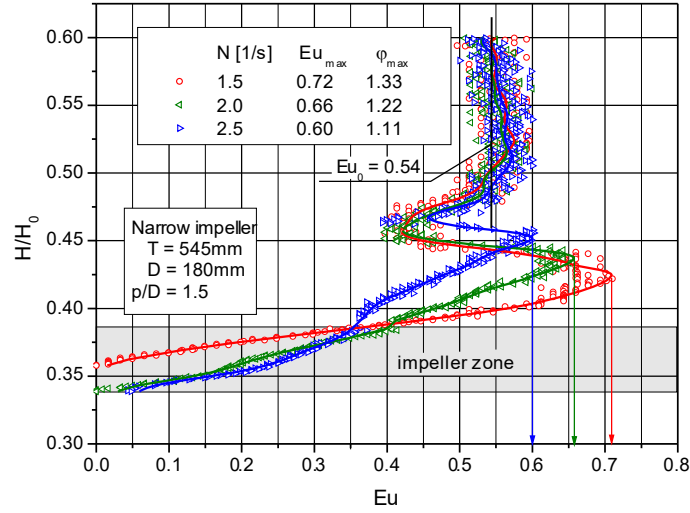

Fig. 6. Euler number increase when emptying the tank for narrow impellers

Previously published papers (Rieger et al., 2019; Stelmach et al., 2020; Rieger et al., 2021) show that the value of the mixing power increase factor depends not only on the type of impeller and its geometric parameters but also on the magnitude of the centrifugal force acting on the liquid in the impeller area, i.e. on the value of the Froude number. This is the main process parameter influencing the value of φ. Therefore, Fig. 7a presents in a double-logarithmic system the experimental points of the relationship $\varphi = f(Fr)$ for propeller impellers with different pitches of the impeller blade p/D. As a result of statistical calculations, straight lines were obtained for individual p/D values with a slope in a narrow range of $-0.388 \div -0.352$, which allows the results of the equation to be correlated with the power function (5), assuming the average value of the exponent at the Froude number Fr in Fig. 7a is equal to -0.365. Fig. 7b shows the values of the constant A in equation (6) depending on the pitch of the impeller blade p/D (legend of Fig. 7b).

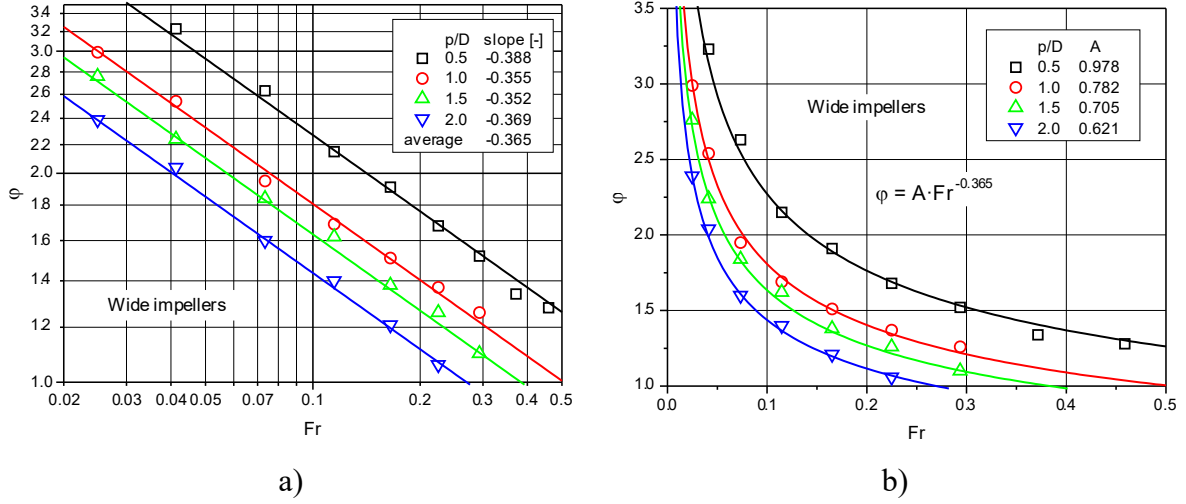$$\varphi = A \cdot Fr^{-0.365} \tag{6}$$

Fig. 7. Values of the power increase factor for wide propeller impellers depending on the Froude number and the impeller blade pitch
a) $\log \varphi = f(\log Fr)$, b) $\varphi = f(Fr)$

Finally, after changing constant A depending on the p/D pitch, equation (6) takes the form of equation (7), and its graphic form is shown in Fig. 7b.

$$\varphi = 0.782 \cdot Fr^{-0.365} \cdot \left(\frac{p}{D}\right)^{-0.315} \pm 2.6\% \tag{7}$$

Using a similar procedure for propeller impellers with narrow blades, equation (8) was obtained which describes the relationship $\varphi = f(Fr, p/D)$. The low values of experimental errors in both correlation relationships should be noted.

$$\varphi = 0.776 \cdot Fr^{-0.197} \cdot \left(\frac{p}{D}\right)^{-0.221} \pm 1.5\% \tag{8}$$

In Fig. 8 the values of the mixing power increase factors φ obtained in this study for propeller impellers were compared with similar values φ obtained for other types of impellers. As can be seen from the analysis of this drawing, wide propeller impellers were characterized by significantly higher φ values than other types of impellers. This most likely results from the fact that these impellers generate the largest vertical stream of liquid flowing through the impeller area (Stelmach et al., 2023) compared to other designs. When changing the direction of liquid flow in the impeller area from axial to radial, the flow direction of the stream is changed to perpendicular in relation to the previous one and additionally, the rotation direction of a large mass of liquid is changed to the opposite. Changing the direction requires supplying additional energy to the system. The greater this stream, the greater the demand for additional energy. However, this problem requires further research.
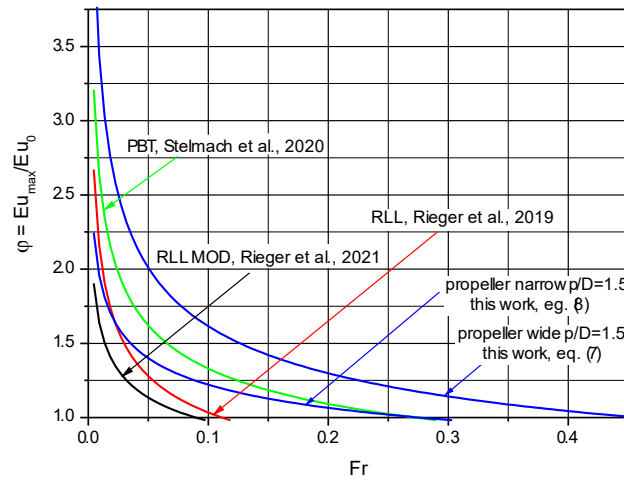
11

Fig. 8. Comparison of mixing power increase factors for different types of axis impellers

According to the works of Regier et al. 2019, Regier et al. 2021, no changes in the mixing power increase coefficients φ were observed with an almost three-fold linear increase in the mixer scale.

6. CONCLUSIONS

1. While the tank is being emptied with the propeller impeller running, the mixing power increases very quickly at the moment when the free surface of the liquid is close to the upper surfaces of the impeller blades.

2. Wide propeller impellers are characterized by the highest mixing power increase rates of all axial mixers.

3. For propeller impellers with wide blades, in the limit case, the mixing power can be as much as three times higher than the mixing power for a full tank.

4. If the tank is big and its emptying rate is slow, the long time during which the motor is subjected to increased load may lead to its burning out.

5. The observed effect of a significant decrease in torque when emptying the tank in the period just before its rapid increase requires further research and analysis.

12

SYMBOLS

B - baffle width, m

C - the height of the impeller suspension above the tank bottom, m

D - the diameter of the impeller, m

H_0 - tank height, m

H - distance of the free surface of the liquid from the bottom, m

H^* - dimensionless distance of the free surface of the liquid from the bottom = H/H_0, -

M - torque, Nm

N - rotational frequency, s^{-1}

P - power, W

R - radius (distance from the impeller axis), m

R_{imp} - impeller radius, m

T - tank diameter, m

U_r, U_z - radial and axial velocity respectively, m/s

U^* - dimensionless velocity = $\sqrt{(u_r^2 + u_z^2)/(\pi DN)}$, -

$\dot{V}$ - volumetric flow rate, m^3/s

h - the current height of the liquid in the tank, m

h^* - dimensionless current height of the liquid in the tank = h/H_0, -

b - the width of the blade, m

g - acceleration due to gravity, m/s^2

p - propeller impeller blade pitch, m

r - radial coordinate, m

z - axial coordinate, m

Greek symbols

α - the angle of inclination of the blades in relation to the horizontal plane, rad

η - viscosity, Pa·s

φ - mixing power increase factor

ρ - density, kg/m^3

Dimensionless numbers

$$\mathrm{Re} = \frac{N \cdot D^2 \cdot \rho}{\eta}$$
    - Reynolds number for mixing process

$$\mathrm{Fr} = \frac{N^2 \cdot D}{g}$$
    - Froude number for mixing process

$$\mathrm{Eu} = \frac{P}{N^3 \cdot D^5 \cdot \rho}$$
    - Euler/power number

Acronims of impellers

FBT - flat blade turbine

PBT - pitched blade turbine

RT - Rushton turbine

RLL - impeller with folded paddles

RLL MOD - modified impeller with folded paddles (with vertical plates at blade tip)

Availability of data and materials: Data obtained during own research were used in the work. Other data that we refer to in the work are available in the publications from which they were taken.

REFERENCES

1. Alberini F., Albano A., Singh P., Christodoulou C., Montane G., Maluta F., Paglianti A., 2024. Fluid dynamics and power consumptions in a single use stirred tank adopted in the pharmaceutical industry. *Chem. Eng. Res. and Design*, 204, 159-171. DOI: 0.1016/j.cherd.2024.02.023.

2. Barresi A., Baldi G., 1987. Solid dispersion in an agitated vessel. *Chem. Eng. Sci.*, 42, 2949-2956. DOI.org/10.1016/0009-2509(87)87060-4.

3. Bates R., Fondy P., Fenic J., 1963. In: *Mixing: Theory and Practice*. (Uhl V. and Gray J., eds.), Vol I, Chap.3. Academic Press, New York, 1966.

4. BN-2472-01:1977. Mieszadła śmigłowe trójłopatkowe spawane D=315÷780 mm. Available at: https://bc.pollub.pl/dlibra/publication/9578/edition/11917.

5. BN-2225-13:1984. Mieszarki pionowe - Mieszadła śmigłowe trójłopatkowe D=200÷800 mm. Available at: https://bc.pollub.pl/dlibra/publication/9123/edition/11721.

6. Furukawa H., Kato Y**.**, Yoshiro Inoue Y., Kato T., Tada Y., Hashimoto S., 2012. Correlation of Power Consumption for Several Kinds of Mixing Impellers, *International Journal of Chemical Engineering*, ID 106496. DOI. 10.1155/2012/106496.

7. Jaworski Z., Nienow A.W., Dyster K.W., 1996. An LDA study of the turbulent flow field in a baffled vessel agitated by an axial, down-pumping hydrofoil impeller. *Canadian Journal of Chemical Engineering*, 74, 3–15. DOI: 10.1002/cjce.5450740103.

8. Kaćunić A., Akrap M., Kuzmanić N., 2013. Effect of impeller type and position in a batch cooling crystallizer on the growth of borax decahydrate crystals. *Chemical Engineering Research and Design*, 91, 274-285. DOI. 10.1016/j.cherd.2012.07.010.

9. Landau J., Procházka J., 1964. Studies of mixing XVII. Relations between the energy consumption and rate of homogenization. *Coll. Czech. Chem. Commun.* 29, 1866-1876.

10. Mak A.T.-Ch., 1992. *Solid-liquid mixing in mechanically agitated vessels*, PhD Thesis, University College London.

11. Mazoch J., 2016. *Provozní měření na aparátu 300 m³*. Projekt TA ČR TH01020879. TECHMIX Brno, 2016. (in Czech)

12. Mersmann A., 2001. *Crystallization technology handbook*. 2nd edition, Marcel Dekker Inc., New York.

13. Nagata S., 1975. *Mixing: Principles and Applications*. John Wiley & Sons, New York.

14. Paul E.L., Atiemo-Obeng V.A., Kresta S.M., 2004. *Handbook of Industrial Mixing*; John Wiley & Sons: Hoboken, NJ.

15. Plewik R., Synowiec P., Wójcik J., Kuś A., 2010. Suspension flow in crystallizers with and without hydraulic classification. *Chem. Eng. Res. and Design* 88, 1194–1199. DOI. 10.1016/j.cherd.2009.08.008.

16. Rane V.C., Ekambara K., Joshi J.B., Ramkrishna D., 2014. Effect of impeller design and power consumption on crystal size distribution. *AIChE J.* 60, 3596–3613. DOI: 10.1002/aic.14541.

17. Reviol, T., Kluck, S., Ettringer, G., Böhle, M., 2018a. Investigation of propeller mixer for agitation of non-newtonian fluid flow to predict the characteristics within the design process. *Chem. Eng. Sci.* 191, 420–435. DOI: 10.1016/j.ces.2018.05.028.

18. Reviol T., Kluck S., Böhle M., 2018b. A new design method for propeller mixers agitating non-Newtonian fluid flow, *Chem. Eng. Sci.* 190, 320–332. DOI: 10.1016/j.ces.2018.06.033.

19. Rieger F., Jirout T., Moravec J., Stelmach J., Kuncewicz C., 2019. The phenomenon of increased mixing power consumption during tank emptying. *Przem. Chem.* 98, 962-966. DOI: 10.15199/62.2019.6.21. (in Polish)

20. Rieger F. , Moravec J., Stelmach J., Kuncewicz C., 2021. Influence of modification of the stirrer with folding blades on the increase of mixing power during emptying the tank. *Przem. Chem.* 100, 1231-1235. DOI: 10.15199/62.2021.12.15. (in Polish)

21. Rushton J., Costich E., Everret H., 1950a. Power characteristics of mixing impellers. *Chem. Eng. Prog.* 46, 395–404.

22. Rushton J., Costich E., Everret H., 1950b. Power characteristics of mixing impellers. *Chem. Eng. Progr.*, 46, 467–474.

23. Sha Z., Palosaari S., 2000. Mixing and crystallization in suspensions, *Chem. Eng. Sci.*, 55, 1797-1806. DOI: 10.1016/S0009-2509(99)00458-3.

24. Stelmach J., Kuncewicz C., Jirout T., Rieger F., 2023. Mixing tank hydrodynamics and mixing efficiency for propeller impellers. *Chemical Engineering Research and Design* 199, 460–472. DOI: 10.1016/j.cherd.2023.09.036.

25. Stelmach J., Kuncewicz C., Szufa S., Jirout T., Rieger F., 2021a. The influence of hydrodynamic changes in a system with a pitched blade turbine on mixing power. *Processes* 9(1), 68. DOI: 10.3390/pr9010068.

26. Stelmach J., Kuncewicz C., Adrian Ł., Jirout T., Rieger F., 2021b. Change of agitation power when emptying the tank for two impellers with axial action. *Processes* 9(2), 341. DOI: 10.3390/PR9020341.

27. Stelmach J., Kuncewicz C., Rieger F., Moravec J., Jirout T., 2020. Increase of mixing power during emptying of tanks with turbine-blade impellers. *Przem. Chem.*, 99, 239–243. DOI: 10.15199/62.2020.2.11. (in Polish)

28. Wang P., Reviol ., Kluck S., Würtz P., Bohle M., 2018. Mixing of non-Newtonian fluids in a cylindrical stirred vessel equipped with a novel side-entry propeller. *Chem. Eng. Sci.* 190, 384-395. DOI: 10.1016/j.ces.2018.06.034.

29. Wylock C., Gutierrez V., Debaste F., Cartage T., Delplancke-Ogletree M.-P., Haut B., 2010. Influence of mixing and solid concentration on sodium bicarbonate secondary nucleation rate in stirred tank: theoretical and experimental studies. *Crystal Research and Technology*, 45, 929-938. DOI: 10.1002/crat.201000233.